

Identification of anti-inflammatory and antimicrobial compounds from leaves and rhizomes of Iris pseudacorus collected in Irland bogland using chemical profiling techniques

Erol, O.; Nagar, S.; Selo, M.A.; Obalidi, I.; Walsh, J.J.; Sheridan, H.; Choi, Y.H.

Citation

Erol, O., Nagar, S., Selo, M. A., Obalidi, I., Walsh, J. J., Sheridan, H., & Choi, Y. H. (2025). Identification of anti-inflammatory and antimicrobial compounds from leaves and rhizomes of Iris pseudacorus collected in Irland bogland using chemical profiling techniques. *Fitoterapia*, 185. doi:10.1016/j.fitote.2025.106671

Version: Publisher's Version

License: <u>Creative Commons CC BY 4.0 license</u>
Downloaded from: <u>https://hdl.handle.net/1887/4283703</u>

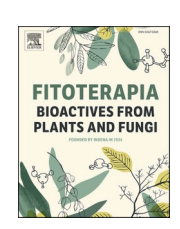
Note: To cite this publication please use the final published version (if applicable).

ELSEVIER

Contents lists available at ScienceDirect

Fitoterapia

journal homepage: www.elsevier.com/locate/fitote





Identification of anti-inflammatory and antimicrobial compounds from leaves and rhizome of *Iris pseudacorus* collected in Ireland bogland using chemical profiling techniques

Özlem Erol ^{a,*}, Shipra Nagar ^b, Mohammed Ali Selo ^{b,c}, Ismael Obaidi ^{b,d}, John J. Walsh ^b, Helen Sheridan ^b, Young Hae Choi ^a

- ^a Natural Products Laboratory, Institute of Biology, Leiden University, Sylviusweg 72, 2333BE Leiden, the Netherlands
- b NatPro Centre, School of Pharmacy and Pharmaceutical Sciences, Trinity College Dublin, Dublin 02, D02 PN40 Dublin, Ireland
- c Faculty of Pharmacy, University of Kufa, Al-Najaf, Iraq
- ^d College of Pharmacy, University of Babylon, Babylon, Iraq

ARTICLE INFO

Keywords: Iris pseudacorus HPTLC bioautography Antimicrobial and anti-inflammatory activity

ABSTRACT

Iris pseudacorus, a species native to Irish wetlands, was investigated for its antimicrobial and anti-inflammatory potential as part of a broader study on bogland medicinal plants. Methanol extracts from leaves and rhizomes were chemically profiled using NMR, LC-MS, and HPTLC, leading to the identification of three bioactive compounds: syringic acid, luteolin 7-O- β -D-glucoside, and liquiritigenin. HPTLC bioautography revealed that these compounds exhibited moderate antimicrobial activity against *Staphylococcus aureus* ATCC 29213, with MIC values ranging from 128 to 256 µg/mL. In vitro anti-inflammatory assays using THP-1 macrophages further demonstrated significant inhibition of interleukin-6 (IL-6) production, particularly by liquiritigenin, which showed the strongest bioactivity in both assays. These findings highlight the therapeutic potential of *I. pseudacorus* and support its traditional use in Irish ethnobotany, offering a promising example of bioactive compound discovery from underexplored wetland flora.

1. Introduction

Iris pseudacorus, commonly known as Yellow Iris or Yellow Flag Iris, is a very common species found in Irish boglands [1]. Classified as an ornamental plant [2], it also has a cultural significance in Irish folklore for its ethnopharmacological uses, including the treatments of coughs, dyspepsia, toothaches, indigestion, and serpent bites [3,4]. Iris pseudacorus is known for its diverse chemical composition, that includes primary and specialised metabolites, such as essential oils, terpenes, saponins, flavones, isoflavones, alkylresorcinols, alkaloids, and xanthones, which are distributed throughout various parts of the plant (flower, stem, leaves, and rhizomes) [5,6]. These compounds have been reported to exhibit a wide range of biological activities, including antiviral [7], anti-biofilm [8], antibacterial [9], cytotoxic [10], butyrylcholinesterase-inhibiting [11], anti-tumor [12,13], and antiosteoporotic activities [14]. The worldwide distribution of Iris species and their significant biological activities have prompted research groups to investigate their metabolic profiles leading among others, numerous reports of the isolation and purification of novel isoflavones from *Iris* rhizomes [15,16].

Interestingly, in addition to its pharmacological applications, *Iris pseudacorus* has been explored for its phytoremediation potential. Rhizomes of *Iris* species have demonstrated the ability to remediate various contaminants from aquatic ecosystems, including pharmaceutical drugs (e.g., furosemide, ibuprofen, methamphetamine, and tramadol) [17–19], pesticides (e.g., imazalil, chlorpyrifos) [20,21], herbicides (e.g., atrazine) [22], and heavy metals such as arsenic, copper, lead, and cadmium [23,24].

The *Iris* genus is notable for its diverse array of secondary metabolites. Plant-derived antimicrobials may provide novel mechanisms of action against resistant pathogens, potentially circumventing current resistance mechanisms. Additionally, plant metabolites with anti-inflammatory properties can modulate LPS-induced inflammatory pathways, offering potential therapeutic benefits for managing inflammation-driven diseases [25]. Exploring these natural compounds not only provides a sustainable and diverse source of novel therapeutics

E-mail address: o.erol@biology.leidenuniv.nl (Ö. Erol).

^{*} Corresponding author.

but also aligns with the growing interest in natural and integrative medicine.

Iris pseudacorus was selected as part of the Irish Bogland project titled "Unlocking Nature's Pharmacy," due to its popularity in Irish folklore for treating ailments such as mumps, jaundice, wounds, sore throats, and burns as mentioned before [3,4,26]. This study aims to explore its chemical diversity and therapeutic potential through a comprehensive metabolomics-guided approach. Sixteen dried plant samples collected from three distinct regions of Ireland were analysed using highperformance thin-layer chromatography (HPTLC), liquid chromatography-mass spectrometry (LC-MS), and nuclear magnetic resonance (NMR) spectroscopy. By integrating chemical profiling with biological assays, this work seeks to evaluate the pharmacological relevance of I. pseudacorus, particularly its antimicrobial and antiinflammatory potential, and to contribute to the broader understanding of native wetland flora as a reservoir of bioactive compounds.

2. Material and methods

2.1. Plant material

Whole plant material (rhizome, leaf and stem) was collected from various locations in Ireland, packed in plastic bags and shipped directly to Dublin or stored chilled until it could be sent. The species was identified by John J. Cannon (Agricultural Adviser with Teagasc – the Irish Agriculture and Food Development Authority) and voucher specimens were deposited in the in-house collection at Trinity College (Ireland, NatPro). Representative voucher samples for the collections were prepared and submitted to the herbarium at the National Botanic Gardens of Ireland, and accession numbers were obtained. Detailed information on the collection of *Iris* samples is listed in Table 1. Once in the laboratory, the plant material was separated according to plant part, that is, rhizomes, leaves and stems, and dried at ambient temperature (10 $^{\circ}$ C – $18\,^{\circ}$ C depending upon the time of collection). Once the material was dry, it was pulverised and separated into sixteen samples that were used for extraction.

2.2. Chemicals and reagents

The chemicals used for extraction and development of (HP)TLC plates, MeOH, EtOAc, toluene and acetone (analytical grade) were purchased from Avantor - Macron Fine Chemicals (Gliwice, Poland), LC-MS grade solvents (AcCN, MeOH, $\rm H_2O$) were purchased from Biosolve (Dieuze, France). Formic acid (LC-MS grade) and sodium formate solution (10 mM NaOH, LC-MS grade) for the calibration were purchased from Sigma-Aldrich (St. Louis, MO, USA). HPTLC silica gel 60 F254 glass plates were purchased from Merck (Darmstadt, Germany), TLC plates silica gel 60 F254 and preparative TLC plates were purchased from VWR Chemicals (Rue Carnot, France). Anisaldehyde (\geq 97 %), sulfuric acid and acetic acid (ACS reagent \geq 96 %) were purchased from Sigma-Aldrich. Purified water was obtained using a Milli-Q system (Millipore, Burlington, MA, United States). For NMR analysis CH₃OH- d_4 solvent were obtained from Eurisotop (Saarbruecken, Germany) and hexamethyldisiloxane (HMDSO) from Fluka (Landsmeer, Netherlands).

2.3. High performance thin layer chromatography (HPTLC) analysis

2.3.1. Extraction of plant material for HPTLC analysis

Thirty mg of dried plant samples were mixed with 5 mL of MeOH (solid-to-solvent ratio of 1:6 (w/v)) followed by 1 min vortexing and 30 min ultrasonication at 25 °C (Branson 5510-MT Ultrasonic cleaner (Branson Ultrasonics, Danbury, USA)). The resulting MeOH extracts were centrifuged for 10 min at a speed of 21,952 g to yield clear supernatants that were separated and dried with a SpeedVac (at 35 °C) (CentriVap Concentrator, LabconcoTM, Kansas City, MO, USA). Five mg of dried extracts were redissolved in 1 mL MeOH for HPTLC analysis.

Table 1Collection information of sixteen *Iris pseudacorus* samples Bogland of Ireland employed in the study.

Voucher Specimens No.	Collection county in Ireland	GPS Co- ordinates (latitude, longitude)	Type of habitat	Collection time	Plant parts ^a
NTP0018	Donegal	54.9831, -7.9734	Blanket bog, Atlantic	September 2020	Rhizom
NTP0021	Donegal	54.9945, -7.9547	type Blanket bog, Atlantic	September 2020	Rhizom
NTP0022A	Donogol	54.9945,	type Blanket bog,	September	Leaf
NIPOUZZA	Donegal	-7.9547	Atlantic type Blanket	2020	Leai
NTP0022B	Donegal	54.9945, -7.9547	bog, Atlantic type	September 2020	Rhizom
NTP0022C	Donegal	54.9945, -7.9547	Blanket bog, Atlantic type	September 2020	Stem
NTP0023A	Donegal	54.9945, -7.9547	Blanket bog, Atlantic type	September 2020	Rhizom
NTP0023B	Donegal	54.9945, -7.9547	Blanket bog, Atlantic type	September 2020	Stem
NTP0023C	Donegal	54.9945, -7.9547	Blanket bog, Atlantic type	September 2020	Leaf
NTP0024A	Donegal	54.9945, -7.9547	Blanket bog, Atlantic type	September 2020	Stem
NTP0024B	Donegal	54.9945, -7.9547	Blanket bog, Atlantic type	September 2020	Leaf
NTP0024C	Donegal	54.9945, -7.9547	Blanket bog, Atlantic type	September 2020	Rhizom
NTP0025A	Donegal	54.9945, -7.9547	Blanket bog, Atlantic type	September 2020	Rhizom
NTP0070	Offaly	53.2780, -7.4923	Fen, wet bog	June 2020	Rhizom
NTP0129	Kildare	53.2784, -6.9430	Raised bog, peatland	June 2020	Leaf
NTP0130	Kildare	53.2784, -6.9430	Raised bog, peatland	June 2020	Rhizom
NTP0131	Kildare	53.2784, -6.9430	Raised bog, peatland	June 2020	Stem

^a The leaves samples possibly contain few stem.

2.3.2. HPTLC performance

For the HPTLC analysis 10 μ L of the extract solution (5 mg/mL) were applied to 200 \times 100 mm HPTLC silica gel 60 F254 glass plates (Merck, Darmstadt, Germany) in 6.0 mm bands with a TLC Sampler (ATS 4, CAMAG, Muttenz, Switzerland). Two different mobile phases: (a) toluene-acetone (1,1, ν / ν) for the separation of non-polar to moderately polar compounds, and (b) EtOAc-formic acid-acetic acid-water (100,11:11:27, ν / ν) for polar compounds were used as mobile phases.

The development was automatically performed in an ADC2 CAMAG 1020 chamber with 35 min saturation time (relative humidity kept at 33 % with a saturated solution of magnesium chloride (Sigma-Aldrich)) and 85 mm solvent migration distance from the sample application point. The developed HPTLC plates were visualised using CAMAG TLC Visualizer, with visible, UV 254 nm, and UV 366 nm light. All the HPTLC plates were sprayed with 2 mL of anisaldehyde-H₂SO₄ reagent using a derivatiser (CAMAG) followed by heating at 100 °C for 3 min with the TLC Plate Heater 3 (CAMAG). The derivatised plates were visualised and photographed using the TLC Visualiser under visible and UV light at 366 nm.

2.4. UHPLC-DAD-QTOF-MS analysis

2.4.1. Extraction of plant material for LC-MS analysis

Twenty mg of dried plant material were extracted with 1 mL of 70 % MeOH (ν/ν), corresponding to a solid-to-solvent ratio of 1:50 (w/ν). The mixture was vortexed for 1 min followed by ultrasonication for 30 min at 25 °C. After extraction, the samples were centrifuged at 21,952 ×g for 10 min. The supernatants were then transferred to 1.5 mL glass tubes and filtered through a 0.2 μ m PTFE membrane filters. Samples were diluted 1:100 for LC-MS analysis.

2.4.2. UHPLC-DAD-QTOF-MS analysis

Samples were used for injection into an UHPLC-DAD-QTOF MS system composed of an, Ultimate 3000 UHPLC (Thermo Scientific, Dreieich, Germany), an OTDF-QII spectrometer with electrospray ionization (ESI) (Bruker, Bremen, German). The separation was performed on a Phenomenex, Kinetex, C18 column (2.1 \times 150 mm, 2.6 μm) (Utrecht, The Netherlands) and eluted with a gradient of 0.1 % formic acid in H2O (solvent A) and 0.1 % formic acid in AcCN (solvent B), from 5 % to 95 % in 40 min. The flow rate was 0.3 mL/min, and the column temperature was maintained at 40 °C. The injection volume was set at 1 μL . The following mass spectrometer settings were used: nebulizer gas 2.0 bar, drying gas 10.0 mL/min, temperature 250 °C, capillary voltage 3500 V and data was collected in positive mode with a scan range of 100–1650 m/z. Sodium formate was used as a calibrant.

2.5. ¹H NMR analysis

2.5.1. Extraction of plant material for ¹H NMR analysis

Thirty mg of dry plant materials were extracted with 1 mL of the deuterated solvent, CH $_3$ OH- d_4 containing 3.93 mM hexamethyldisiloxane (HMDSO) as an internal standard or in 1 mL of a mixture of CH $_3$ OH- d_4 and KH $_2$ PO $_4$ buffer in D $_2$ O (1:1, v/v) and 0.29 mM trimethylsilyl propionic acid sodium salt- d_4 (TMSP), followed by 1 min ultrasonication at 25 °C. The extracts were centrifuged at 18928 g, and 300 μ L of the solutions were transferred to 3 mm NMR tubes for 1 H NMR analysis.

2.5.2. ¹H NMR analysis

The 1H NMR analysis was performed with an AV-600 MHz NMR spectrometer (Bruker, Karlsruhe, Germany), operating at the 1H NMR frequency of 600.12 MHz. For internal locking, $CH_3OH\text{-}d_4$ was used. All 1H NMR data consisted of 128 scans requiring 10 min and 26 s as the acquisition time using the parameters: 0.16 Hz/point, pulse width (PW) = 30° (11.3 μs), and relaxation time of 1.5 s. A pre-saturation sequence was used to suppress the residual water signal, using low-power selective irradiation at H_2O frequency during the recycle delay. The FIDs were Fourier transformed with an exponential line broadening of 0.3 Hz. The resulting spectra were manually phased, baseline corrected and calibrated to HMDSO at 0.06 ppm using TOPSPIN V. 3.0 (Bruker).

2.6. GC-MS analysis

2.6.1. Extraction of plant material for GC-MS analysis

Aqueous methanolic extracts were prepared by extraction 30 mg of the plant materials with 1 mL of MeOH-H₂O (1:1, ν/ν), 10 s vortexing and 20 min ultrasonication at 25 °C. The extracts were centrifuged for 10 min at 18928 g. Three hundred μ L of supernatant was transferred to a 1.5 mL glass vial and dried in a Speed vac (at 35 °C). The dried extracts were redissolved in 100 μ L of methoxyamine hydrochloride solution in pyridine (20 mg/mL) and reacted at 40 °C for 2 h. The reactants were then TMS-derivatised by the addition of 140 μ L of *N*-Methyl-*N*-(trimethylsilyl)trifluoroacetamide (MSTFA) and heating at 40 °C for 2 h.

2.6.2. GC-MS analysis

The GC–MS analysis was performed on an Agilent 8890 A gas chromatograph coupled to a 7890 MS system gas equipped with a 7693 automatic sampler (Agilent, Folsom, CA, USA). The samples were analysed using a DB-5 GC column (30 m \times 0.25 mm, 0.25 μm film, J&W Science, Folsom, CA, USA) and eluted with helium (99.9 % purity) as a carrier gas at a flow rate of 1.5 mL/min. The oven temperature was programmed as follows: after an initial hold at 60 °C for 1 min it was, increased at 7 °C /min to 290 °C, and held for 5 min; then increased to 310 °C at 5 °C /min and held for 3 min. The injector was set at 280 °C and 1 μL of the sample was injected in splitless mode. The interface temperature was set at 280 °C, and the ion source and quadrupole temperature were 230 °C and 150 °C, respectively. The ionization energy in EI mode was 70 eV.

2.7. Microdilution antibacterial assay

2.7.1. Extraction of plant material for microdilution antibacterial assay

Thirty mg of dried plant samples were mixed with 5 mL of MeOH (solid-to-solvent ratio of 1:6 (w/v)) followed by 1 min vortexing and 30 min ultrasonication at 25 °C. The MeOH extracts were centrifuged for 10 min at a speed of 21,952 g to yield clear supernatants that were dried using a SpeedVac (at 35 °C). All 16 dried *Iris* extracts were dissolved in 100 % DMSO at a concentration of 10 mg/mL.

2.7.2. Microdilution antibacterial assay

The broth microdilution method was used to determine the minimal inhibitory concentration (MIC) of the tested metabolism according to the Clinical Laboratory Standards Institute guideline (CLSI) [27]. The strains Staphylococcus aureus ATCC 29213, Bacillus cereus and Escherichia coli were inoculated on Mueller-Hinton-Agar (MHA) plates and incubated overnight at 37 °C. From the overnight cultures a single colony was used to inoculate 5 mL of Mueller-Hinton-Broth (MHB) and incubated at 37 °C with constant agitation (180 rpm) overnight. The bacterial suspensions were further adjusted with the addition of MHB to 0.5 of turbidity of the McFarland scale (106 CFU/mL). For testing the extracts were further diluted with MHB a range of in concentrations 512 μg/mL to 16 μg/mL. A volume of 100 μL was added in each well, and $100~\mu L$ of the 0.5~McFarland bacterial suspensions were inoculated into each one and incubated for 24 h at 30. The final concentration of DMSO in the well was below 5 % which was also used as a negative control while 100 μg/mL of spectinomycin was used as a positive control. The bacterial growth was measured by optical density at 600 nm i°Cn a wellmicrotiter plate reader (SPARK 10 M, TECAN, Männedorf, Switzerland) or by visual inspection. The MIC value was defined as the lowest concentration of a compound that completely inhibited bacterial growth at 24 h. All experiments were performed by triplicates. Gram-positive bacteria, Staphylococcus aureus ATCC 29213 and Bacillus cereus, as well as gram-negative bacteria, Escherichia coli were tested in this analysis.

2.8. Direct bioautography using HPTLC plates

A mobile phase consisting of toluene-acetone (1:1, v/v) was selected

for the HPTLC separation used for bioautography, based on its optimal resolution and the absence of acid or any other constituent which might influence the antimicrobial activity in a negative way. Three active samples, voucher specimens No: NTP0024B, NTP0070 and NTP0130 were submitted for analysis. The extracts were applied to the silica gel 60 F254 plates (10 cm \times 5 cm) which were dried for 24 h to completely remove traces of organic solvents after development. A bacterial colony of S. aureus ATCC 29213 was inoculated into 5 mL of M-H broth (pH 7.2) \pm 0.2) and incubated at 37 $^{\circ}\text{C}$ overnight (the mean bacterial concentration was 1.2×10^7 CFU/mL). The bacterial suspension obtained from the overnight incubation was diluted with M-H broth (pH 7.2 \pm 0.2) in a 1: 200 ratio. One hundred microliters of the diluted suspension were added to 10 mL of fresh M-H broth and incubated at 37 °C for approximately four hours. The bacterial mean concentration was 8.0×10^7 (CFU/mL) which corresponds to the logarithmic growth phase. After this, the HPTLC plates were dipped for approximately 15 s in the specified bacterial suspension (S. aureus ATCC 29213). The plates were then placed in a moistened petri dish lined with humid paper and incubated at 37 °C for 24 h. The visualisation of the HPTLC plates was carried out using 0.2 % MTT aqueous solution. Dehydrogenases of living microorganisms reduce MTT to purple formazan. In the places where flumequine standards were applied, white inhibition zones were observed on the purple background. After spraying, the plates were incubated for 4 h at 37 °C [28]. To detect the bands with antimicrobial activity in parallel, a second plate was developed using the same mobile phase. After development and visualisation with the CAMAG TLC Visualiser (under visible or white light, UV 254 nm and UV 366 nm), the plate was sprayed with 1 mL of anisaldehyde-H₂SO₄ reagent using a derivatiser (CAMAG) and placed on a TLC Plate Heater 3 (CAMAG) at 100 °C for 3 min. The derivatised plates were visualised using a CAMAG TLC Visualiser under white and UV light at 366 nm.

2.9. Preparative thin layer chromatography isolation of targeted compounds

Fifty mg of dry plant material from the selected samples (voucher specimens No: NTP0024B, NTP0070 and NTP0130) were extracted similarly to that described in section 2.8. Following the HPTLC bioautography results the samples were spotted manually on 20 \times 10 cm preparative TLC silica gel 60 F254 plates (Merck, Darmstadt, Germany) and developed using toluene: acetone (1:1 v/v) as a mobile phase. The individual zones that exhibited activity in the HPTLC bioautographic test were scraped from the TLC plates. To remove silica gel from the isolated compounds the samples were treated with 5 mL of methanol in Eppendorf tubes and ultrasonicated for 10 min, followed by centrifugation at 10000 g for a further 10 min. This was done for each band by triplicate. After centrifugation, the remaining supernatants were dried and redissolved in 300 μl of MeOH and filtered with 0.20 μm membrane filters before UHPLC-QTOF MS analysis. Compounds were annotated by comparison of their exact mass with the Dictionary of Natural Products, with literature [https://dnp.chemnetbase.com/chemical/ChemicalS earch.xhtml?dswid=7021] using the GNPS and Metaboscape search or comparison by standards. A threshold of 10 ppm was set as the mass error for possible matches. Finally the identity of the compounds was then confirmed by comparison with reference substances.

2.10. Cell culture and treatment

Human monocytic leukaemia THP-1 cells obtained from American Type Culture Collection (ATCC) were maintained in tissue culture flasks (Greiner Bio-One, Frickenhausen, Germany) in a humidified atmosphere at 37 °C, 5 % CO₂ using RPMI 1640 medium (Gibco, Life Technologies, Carlsbad, CA, USA) supplemented with 10 % Fetal Bovine Serum (FBS) (Sigma-Aldrich, Dublin, Ireland). For all experiments, cells were seeded at a density of 5×10^5 cells/mL in 96-well plates. Phorbol 12-myristate 13-acetate (PMA) was added (at a final concentration of 60 ng/mL) to

differentiate the cells from macrophages, after which cells were incubated for 48 h. After this, cells were treated either with 10, 50 and 100 $\mu g/mL$ of one of the *Iris* extracts (voucher specimens No: NTP0024B, NTP0070, NTP0130, NTP0131) or 10, 50 and 100 μM of one of the standard compounds (i.e. syringic acid, liquiritigenin and luteolin 7-O- β -D-glucoside) for 24 h in the presence or absence of lipopolysaccharide (LPS) (ENZO, Farmingdale, NY, USA) which was added after 2 h (at a final concentration of 200 ng/mL). The control cells were treated with 0.2 % DMSO (Sigma-Aldrich, Dublin, Ireland).

2.11. Cells viability assay

Following 24 h incubation with the relevant extract or standard compounds, media supernatants were transferred into new 96-well plates (to be used for cytokine levels analysis, see below). The cells, on the other hand, were incubated with resazurin solution (Assay Genie, Windsor Pl, Dublin 2, Ireland). One hundred microliter of resazurin solution (prediluted with RPMI 1640 at 1:10 ratio) were added per each well and the cells were incubated at 37 °C for 90 min. Afterwards, fluorescence was measured using a SpectraMax M2 plate reader (Molecular device, Sunnyvale, CA, USA) at excitation and emission wavelengths of 544 nm and 590 nm, respectively.

2.12. Analysis of cytokines levels

The levels of four proinflammatory cytokines (i.e., tumor necrosis factor-alpha (TNF- α), interleukin (IL)-6, IL-1 β and Rantes) were measured in the media supernatants collected from cells treated with various extracts and standard compounds using highly binding 96-well plates (SPL Life Sciences, Geumgang, Naechon-Myeon, Korea) and ELISA kits (R&D Systems, Minneapolis, MN, USA) according to the manufacturer's instructions. The supernatant was diluted at 1:20 using Phosphate buffered Saline (PBS) containing 1 % Bovine Serum Albumin (BSA) (Sigma-Aldrich, Dublin, Ireland). To detect the reaction, 3,3′,5,5′-tetramethylbenzidine (TMB) (BD Biosciences, San Jose, CA, USA) solution was added and the plates were incubated for a few minutes before terminating the reaction with diluted 5.4 % sulfuric acid. The absorbance was then measured at 450 nm and subtracted from 540 nm using a SpectraMax M2 plate reader (Molecular device, Sunnyvale, CA, USA).

2.13. Data analysis

The ¹H NMR spectra were bucketed using AMIX 3.9.12 (Bruker BioSpin GmbH, Rheinstetten, Germany) with 0.04 ppm in the range of δ $10.0 - \delta$ 0.3. The integral of each bucket was normalized to total intensity. The normalized buckets were scaled by Pareto scaling method for principal component analysis (PCA) and orthogonal partial least square modelling -discriminant analysis (OPLS-DA) but unit-variance (UV) scaling method was applied to partial least square modelling discriminant analysis (PLS-DA). The UHPLC-MS data were processed and analysed using Bruker Compass Data Analysis software (Bruker). The raw data files were converted to mzML using MSconvert software (Proteowizard) [29]. The quantification table was generated after processing the raw data in mzMine3 [30], and this table was subsequently used for further processing in GNPS. The quantification table obtained from GNPS was then used for multivariate data analysis (MVDA). A library search was performed using MetaboScape [31] and GNPS [32]. MS data are available in the Mass Spectrometry Interactive Virtual Environment (MassIVE) repository MSV000097995. MN workflows can be accessed in GNPS2 with the following links: https://gnps2.org/status? task = f2e66d763cb64192be5c7bf08dadaf6c.

The GNPS results can be accessed by the following link.

The GC-MS raw data files were converted to mzML format using MSconvert software (Proteowizard). The mzML files were processed in Mzmine 2.93. A molecular network was created with the Library Search/Molecular Networking GC workflow at GNPS [33]. The data was

filtered by removing all MS/MS fragment ions within +/-17 Da of the precursor m/z. MS/MS spectra were window filtered by choosing only the top 6 fragment ions in the +/-50 Da window throughout the spectrum. The precursor ion mass tolerance was set to 20,000 Da and the MS/MS fragment ion tolerance to 0.5 Da. The quantitative table obtained from GNPS was used for MVDA. Multivariate data analysis including PCA, PLS-DA, and OPLS-DA were performed using SIMCA P (v.18 Umeå, Sweden).

All data for anti-inflammatory activity were analysed using Graph-Pad prism 8.0 (Graph Pad software, San Diego, CA, USA). Where appropriate, two-way ANOVA followed by Dunnett's multiple comparisons test was used to determine the degree of significance. Results are expressed as means \pm standard deviations (SD). A p-value \leq 0.05 was considered statistically significant.

3. Results and discussion

3.1. Chemical profiling by multi-analytical platform (¹H NMR, HPTLC, UHPLC-MS and GC-MS)

A multi-analytical platform was employed to comprehensively investigate the chemical composition and metabolomic variability of *Iris pseudacorus* samples, combining ¹H Nuclear Magnetic Resonance (¹H NMR), High-Performance Thin Layer Chromatography (HPTLC), Ultra-High Performance Liquid Chromatography-Mass Spectrometry (UHPLC-MS), and Gas Chromatography-Mass Spectrometry (GC–MS). The experimental design involved the collection of sixteen *I. pseudacorus* samples from three distinct regions of the Irish Bogland; Donegal, Offaly, and Kildare. Material from three plant organs (leaves, stems, and rhizomes) from across these regions were examined to assess intra-plant and geographical metabolic differences. The samples were first subjected to broad chemical extraction protocols using different solvent

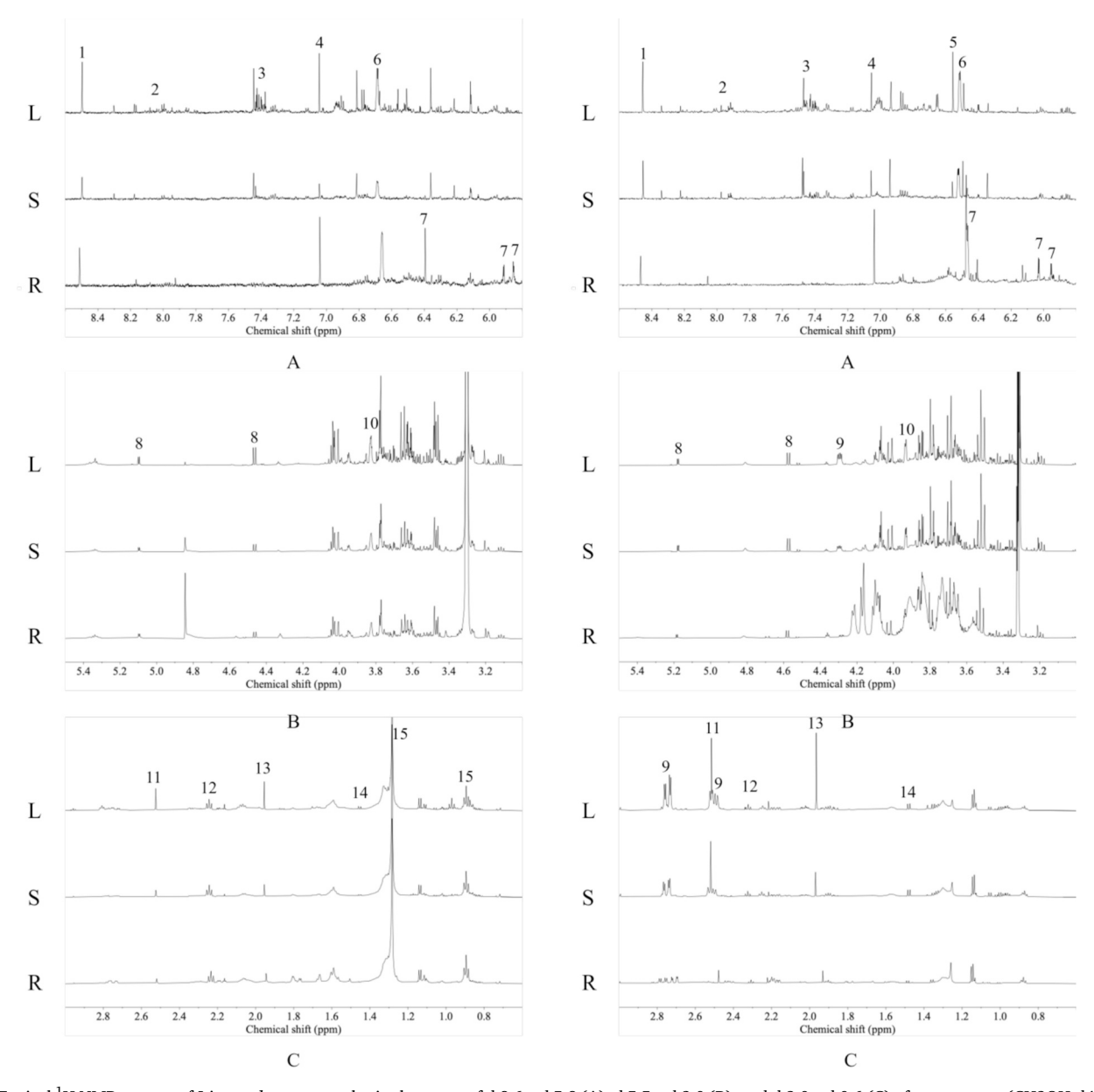


Fig. 1. Typical ¹H NMR spectra of *Iris pseudacorus* samples in the range of d 8.6 – d 5.8 (A), d 5.5 – d 3.0 (B), and d 3.0 – d 0.6 (C) of two extracts (CH3OH-d4 and the mixture of CH3OH-d4 and KH2PO4 buffer in D2O (1:1, v/v). L: leaves, S: stems, R: rhizomes. 1: formic acid, 2: isoflavonoids, 3: luteolin and quercetin, 4: gallotannins, 5: fumaric acid, 6: shikimic acid, 7: flavanones and gallocatechin, 8: glucose, 9: malic acid, 10: fructose, 11: succinic acid, 12: GABA, 13: acetic acid, 14: alanine, 15: fatty acids and lipids.

systems to cover a wide polarity range. Subsequently, analytical data from ¹H NMR, GC–MS, and UHPLC-MS were acquired and subjected to multivariate data analysis (PCA, OPLS-DA, and PLS-DA), supported by molecular networking via the GNPS platform, to identify key metabolites responsible for variations in plant parts and geographical origin. The chemical profiles generated were later correlated with bioactivity data (antimicrobial and anti-inflammatory) to explore structure—activity relationships.

The chemical profiles of the 16 *I. pseudacorus* samples obtained using multiple analytical platforms, including ¹H NMR, HPTLC, UHPLC, and GC–MS were expected to reveal substantial metabolic variation due to environmental factors in different regions of the Irish Bogland (Donegal, Offaly, and Kildare) as well as differences between plant parts (leaves, rhizomes, and stems).

As a first step, ¹H NMR analysis was employed to obtain an overall chemical profile of the *Iris* samples. Two extraction solvents were used to detect a broader range of metabolites: CH₃OH-d₄ for less polar metabolites and a mixture of CH₃OH-d₄ and KH₂PO₄ buffer in D₂O (1:1, ν/ν) for more polar metabolites. The major metabolic differences between samples were attributed more to the plant parts rather than to the collection locations. As demonstrated in Fig. 1, CH₃OH-d₄ extracts showed higher levels of phenolics and lipids, while sugars, amino acids, and organic acids were more prevalent in extracts from the mixture of CH₃OH-d₄ and KH₂PO₄ buffer.

Visual inspection of the 1 H NMR spectra revealed notable metabolic differences between plant parts (leaves, stems, and rhizomes) (Fig. 1). In general, leaves exhibited higher levels of phenolics, particularly isoflavones and flavones (e.g., luteolin and quercetin analogues). For instance, 1 H resonances for H-2 of isoflavonoids around δ 8.0 (s) and H-2′, H-5′, and H-6′ of luteolin and quercetin analogues were more evident in leaves and stems (Fig. 1A). In contrast, two distinct H-6 and H-9 resonances around δ 6.0 – δ 5.8 were more intense in the rhizomes (Fig. 1A). In addition, several primary metabolites, including glucose, fructose, malic acid, succinic acid, formic acid, shikimic acid, acetic acid, alanine, γ -aminobutyric acid (GABA), and fatty acids (lipids), were detected as major constituents in the *Iris* samples.

To further explore metabolic variations, the obtained ¹H NMR spectra were subjected to multivariate data analysis. The spectra from both extraction methods CH₃OH-*d*₄ and the mixture of CH₃OH-*d*₄ and KH₂PO₄ buffer) were combined to provide a comprehensive metabolite dataset comprising 486 variables (243 variables for each extract). Principal component analysis (PCA) was applied to this dataset (Fig. 2A), revealing two factors influencing the Iris metabolome: environmental conditions from the collection sites and internal factors associated with plant parts (leaves, stems, rhizomes). The PCA score plot indicated that internal variation between plant parts was greater than environmental variation and metabolomes of leaves and stems in particular were distinct from those of rhizomes.

Orthogonal partial least squares discriminant analysis (OPLS-DA) was subsequently applied to evaluate the influence of these factors. Three classes (leaves, stems, rhizomes) and two collection locations (Donegal, Kildare) were compared, with one Offaly sample excluded due to its low sample number (Fig. 2B, C). Both models were validated by permutation tests, yielding high Q^2 values (0.49 for plant parts and 0.86 for collection locations).

From both PCA and OPLS-DA, it was confirmed that the metabolome of *Iris* samples was significantly influenced by both plant part and geographic origin. To identify which metabolites were associated with each factor, shared and unique structures (SUS) plots were generated to combine the two OPLS-DA models. As depicted in Fig. 3, ¹H resonances aligned with each axis correspond to metabolites affected by specific factors. Metabolite identification based on H NMR spectra revealed that flavones, isoflavones, malic acid, and glucose were marker metabolites for leaves and stems, while flavanones, fructose, and shikimic acid were markers for rhizomes. Fatty acids and lipids were associated with Donegal samples, and sugars and oxygenated fatty acids assumed form the

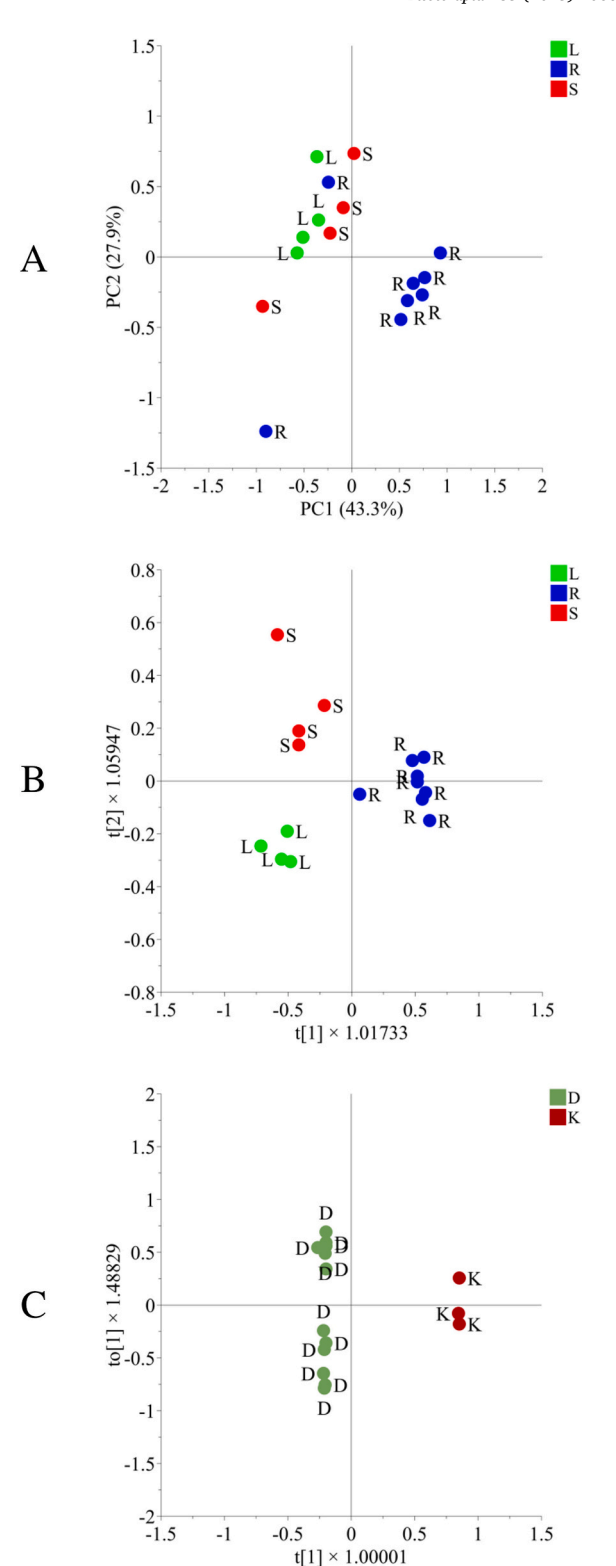


Fig. 2. Score plot of principal component analysis of ¹H NMR data (A), orthogonal partial least square-discriminant analysis modelling using three classes (L: leaves, S: stems, and R: rhizomes) and two classes (D: Donegal and K: Kildare).

resonances in the rage of δ 4.5 – δ 3.5 were characteristic of Kildare samples.

Following this comprehensive investigation of metabolic variations using ¹H NMR, two MS -based profiling techniques were applied to the same dataset: GC–MS for primary metabolites and UHPLC-MS for

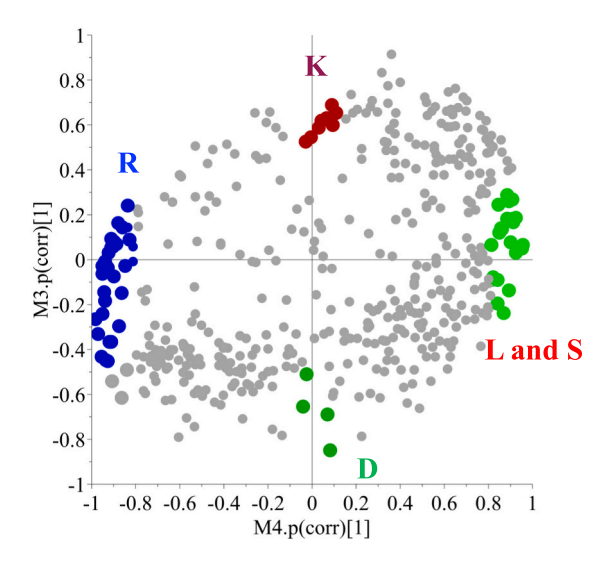


Fig. 3. SUS-plot to combine two orthogonal partial least square-discriminant analysis modelling (x-axis: leaves (L) -stems (S) and rhizomes (R), y-axis: collection in Donegal (D) and Kildare (K)).

specialised metabolites.

In the GC–MS chromatograms, a total of 108 metabolites were identified, as listed in Supplementary Table 1. The GC–MS data were analysed using PCA and OPLS-DA, similar to the approach applied to the ¹H NMR data, to identify marker metabolites associated with different plant organs (leaves, stems, and rhizomes) and collection locations (Kildare and Donegal). The overall results were consistent with the ¹H NMR results. Major metabolic variations were predominantly attributed to plant organs, as shown in the PCA, while both plant organs and collection locations were contributing factors to variations in the OPLS-DA.

The marker compounds distinguishing leaves and stems from rhizomes identified via GC–MS were tagatose, glucaric acid, allantoin, fumaric acid, fructose, trehalose, succinic acid, and \emph{myo} -inositol. In contrast, glucosamine, melizitose, loganin, alanine, β -hydroxymyristic acid, and xylose were identified as markers for rhizomes However, few distinct metabolites were detected in the SUS-plot from the GC–MS analysis of samples according to their collection locations.

In addition to the GC–MS analysis, UHPLC-MS was applied to the same data set to investigate the metabolic difference, especially for specialised metabolites.

To identify metabolites within the samples, UHPLC-MS data were also analysed using feature based molecular networking via the GNPS platform. Supplementary Fig. 1 provides an overview of the molecular networking analysis of UHPLC-MS data in positive mode. Considering all the *Iris* samples, 73 metabolites were annotated, encompassing a range of chemical classes including flavonoids, isoflavonoids, xanthones, alkaloids, coumarins, small peptides, phenolic acids, fatty acids, and di- and triterpenoids. Notably, compounds such as genistein, 5,6,7-trihydroxy-4'-methoxyflavone, and hispidulin were tentatively identified in samples voucher specimens No: NTP0070 (rhizome) and voucher specimens No: NTP0131 (stem). Most identified flavonoids were corroborated by previous reports on *Iris* studies [34]. A complete list of annotated compounds, including those from both positive and negative mode analyses, is available in the supplementary materials (Supplementary Table 2).

As observed in the ¹H NMR and GC–MS analyses, greater variations were noted between plant organs rather than between collection locations. In the PCA score plot (Fig. 4A), leaves (green), stems (red), and rhizomes (blue) were distinctly separated by PC2, though the primary factor driving the variation in PC1 could not be identified. The UHPLC-MS data processed through mzMine and GNPS were further analysed

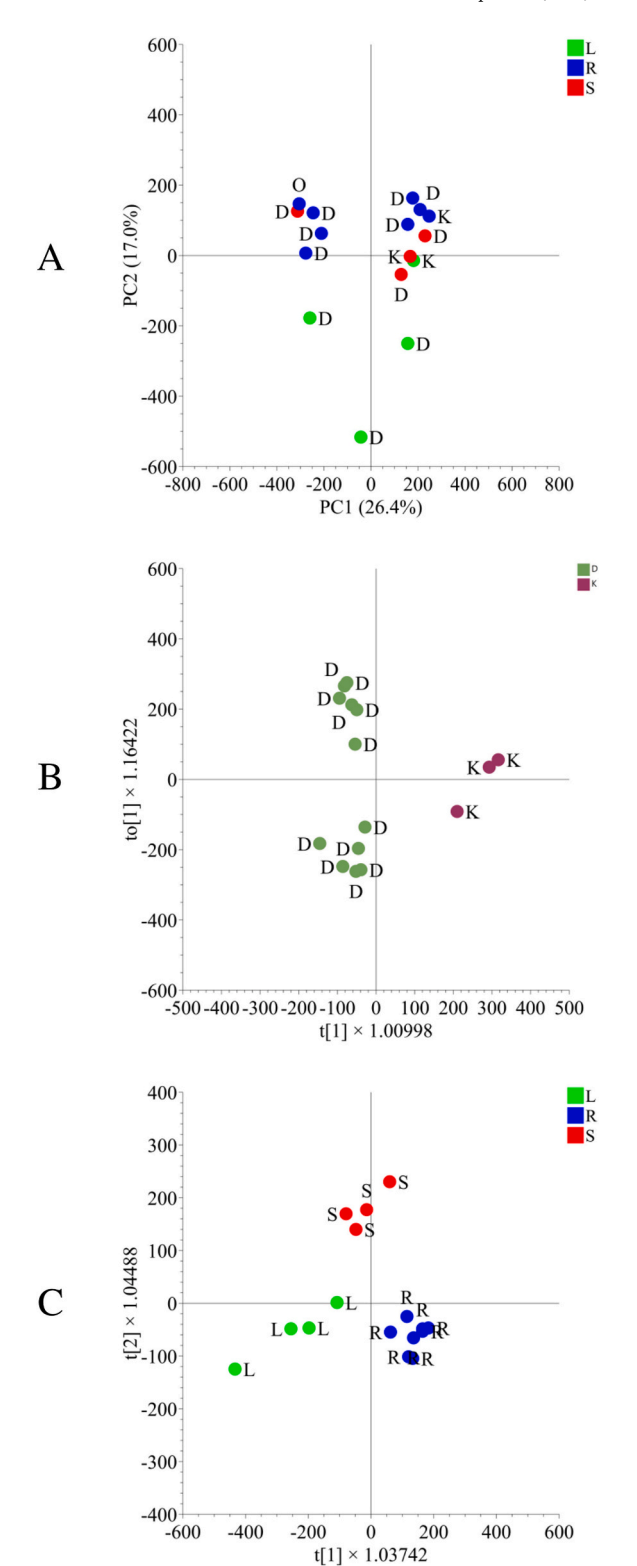


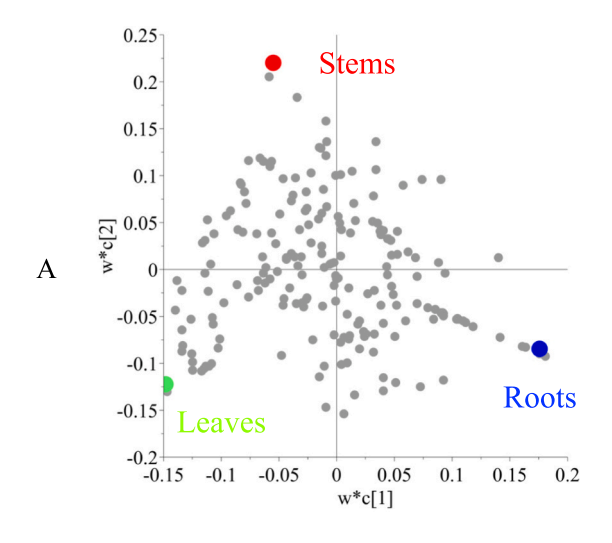
Fig. 4. Score plot of principal component analysis of UHPLC-MS data (A), orthogonal partial least square-discriminant analysis modelling using three classes (L: leaves, S: stems, and R: rhizomes) and two classes (D: Donegal and K: Kildare). In PCA score plot (A), coloring is based on plant organs (leaves, stems, and rhizomes) but labelling on collection places (Donegal and Kildare).

using OPLS-DA, following the same methodology applied to the ¹H NMR and GC–MS data. Both factors contributed significantly to the variation observed, as shown in Fig. 4B and C, confirmed by permutation tests. Stems were clearly differentiated from leaves, though stems and leaves

were clustered closely in the $^1\mathrm{H}$ NMR and GC–MS data. In terms of collection locations, samples from Donegal and Kildare were distinctly separated, consistent with the results from the $^1\mathrm{H}$ NMR and GC–MS analyses.

To identify marker compounds associated with each factor, PLS-DA loading plots were applied to the UHPLC-MS dataset, instead of using the SUS-plot from the combined OPLS-DA for ¹H NMR and GC-MS. Marker compounds were identified for leaves, stems, and rhizomes (Fig. 5A), as well as for samples collected from Donegal and Kildare (Fig. 5B).

Notably, a metabolite which was significantly high in leaves was identified as 2-carboxyarabinitol (molecular ions at m/z 197), a compound reported in the leaves of numerous C3 plants [35]. This compound plays a role in photosynthesis. A second molecular ion at m/z 174 was also characteristic for leaves, but unfortunately, these compounds could not be further characterised by database and literature search. In stems the marker compound was identified by the molecular ion [M-H]⁺ at m/z 298 as a isoflavonoid(5,7-dihydroxy-6-methoxy-2,17-dioxatetracyclo[8.7.0.0³, ⁸.0¹¹, ¹⁶]heptadeca-1(10),3,5,7,11(16),12,14-heptaen-9-one) which had been already described for *Iris pseudacorus* [36]. In rhizome extracts, three molecular ions were detected and identified as potential marker compounds. One of these markers was identified as epicatechin, with a molecular ion at m/z 291. The other two molecular



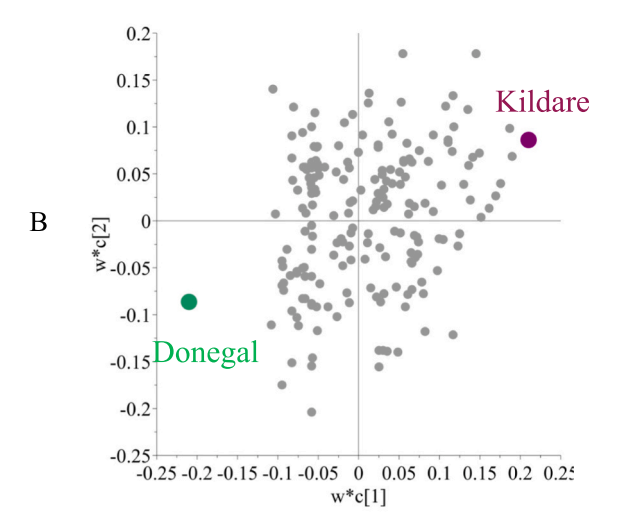


Fig. 5. Loading plot of partial least square modelling – discriminant analysis using three classes of leaves, stems and rhizomes (A), and two classes of Donegal and Kildare (B).

ions, at m/z 611 and m/z 915, were clustered within the procyanidin B2 molecular family in the GNPS network. Based on this clustering and structural similarity, these molecular ions it was considered likely that they represented procyanidin-like compounds. Therefore, the marker compounds identified in the rhizomes are probably tannins, specifically procyanidins and related flavonoids (Fig. 6). Regarding collection locations, the compounds irisolidone (molecular ion m/z 315) and methyl syringate (molecular ion m/z 213) were identified as markers for the Kildare samples, while no specific metabolites were closely associated with Donegal samples.

To investigate the biological activities of *I. pseudacorus* samples and to correlate these with chemical profiling data, antimicrobial and antiinflammatory activities were assessed based on previous studies [34,37].

3.2. Antimicrobial activity of Iris pseudacorus samples and identification of active metabolites

3.2.1. Antimicrobial activity of Iris pseudacorus samples

Methanol extracts of *Iris pseudacorus* were tested for their antimicrobial activity against two Gram-positive bacterial strains—*Staphylococcus aureus* ATCC 29213 and *Bacillus cereus*—as well as one gram-negative strain, *Escherichia coli*. The antimicrobial activity was evaluated using the broth microdilution method in accordance with CLSI guidelines, allowing for the determination of the minimum inhibitory concentration (MIC). Among the sixteen extracts derived from different plant parts and collection sites, three samples demonstrated moderate inhibitory effects against the gram-positive strains, with MIC values below 256 $\mu g/mL$. These included the methanol leaf extract from Donegal (NTP0024B) and the methanol extracts of rhizome collected from Offaly (NTP0070) and Kildare (NTP0130).

These results suggest a selective antimicrobial potential of $\it I. pseudacorus$ methanol extracts against gram-positive bacteria, as no significant inhibition was observed against $\it E. coli.$ Further phytochemical investigation was therefore undertaken to identify the bioactive constituents responsible for the antimicrobial effects observed in the active samples.

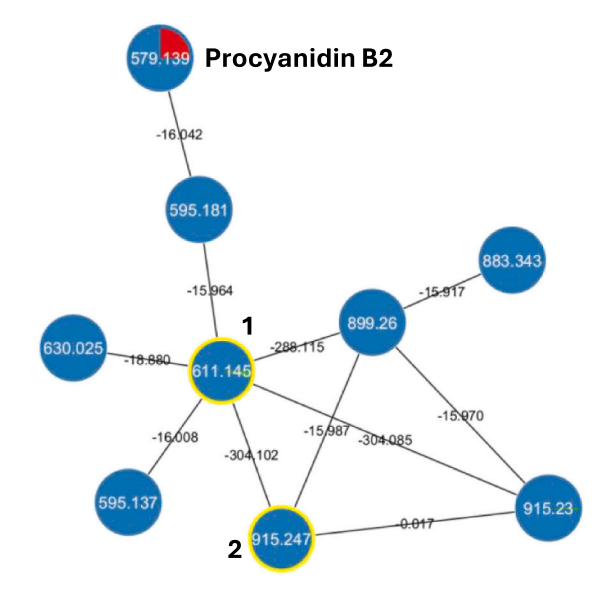
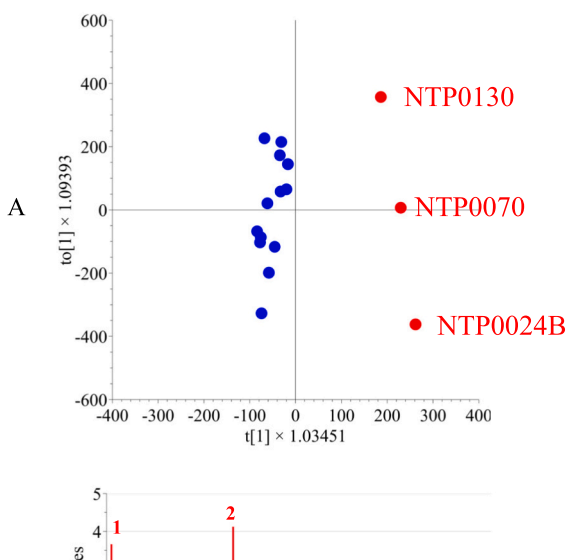


Fig. 6. Two molecular ions in LC-MS data were identified as potential markers for rhizomes. The molecular ions at m/z 611 (1) and 915 (2) clustered within the procyanidin B2 family in the GNPS network, suggesting they are procyanidin-like compounds. Blue represents root samples and red represents leave samples. (For interpretation of the references to colour in this figure legend, the reader is referred to the web version of this article.)

3.2.2. Identification of active metabolites

For the identification of metabolites responsible for the activities, OPLS-DA using two classes (active and non-active) were applied to ¹H NMR, UHPLC-MS, GC-MS data. All the models showed low Q2 values (< 0.4), which might be due to the lack of sample numbers. Nevertheless UHPLC-MS data showed an interesting separation (Fig. 7A). The higher peaks in UHPLC-MS chromatograms of active samples were identified by comparing active and non-active samples (Fig. 7B). Two UHPLC-MS features were clearly shown to be higher in the active samples and one of the features was identified as a isoflavonoid, irisolidone (4'-Omethoxytectorigenin) by molecular networking. After identification the antimicrobial metabolites by correlating between chemical profiling data and activity, the samples were subjected to a further separation to isolate the active compounds. For this, high performance thin layer chromatography (HPTLC) was applied to the samples. In the field of metabolomics and chemical profiling, HPTLC has been often used for a preparative purpose to isolate target compounds from a minimum sample size at high speed and also for chemical fingerprinting [38,39].

The results of 1 H NMR and UHPLC-MS indicated that some flavonoids might be responsible for the antimicrobial activity. In view of this two mobile phases, toluene-acetone (1:1, ν / ν) and EtOAc-formic acidacetic acid-water (100:11:11:27, ν / ν) were chosen for the separation. The acid-free mobile phase, toluene-acetone (1:1, ν / ν) was used for bioautography, in which HPTLC chromatograms were directly tested by bacterial growth (Fig. 8). The three active samples (voucher specimens



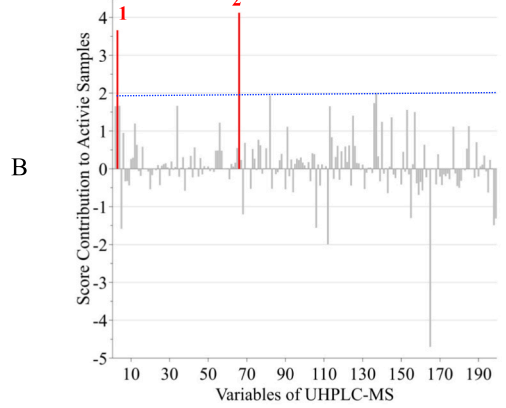


Fig. 7. Score plot of orthogonal partial least square-discriminant analysis modelling modelling using two classes (active in red and non-active in blue) (A) of UHPLC-MS data and increased UHPLC-MS variables compared to the average variables of all the tested samples (B). 1: Unknown at m/z 219.018, 2: irisolidone (4'-O-methoxytectorigenin). (For interpretation of the references to colour in this figure legend, the reader is referred to the web version of this article.)

No: NTP0024B, NTP0070, and NTP0130) were subjected to direct bio-autography to identify the active compounds. Fig. 9 presents the results of the bioautography assay, showing the zone of inhibition against S. aureus ATCC 29213. For voucher specimens No: NTP0024B an R_f value of 0.75, and for voucher specimens No: NTP0130, an R_f value of 0.85 indicated inhibition zones. For voucher specimens No: NTP0070, three distinct inhibition zones were detected with R_f values of 0.65, 0.7, and 0.88.

The active bands revealed on the HPTLC bioautography were isolated by preparative TLC and analysed by UHPLC-MS to identify their chemical structures. These compounds were identified as liquiritigenin, syringic acid, and luteolin 7-O-D-glucoside in voucher specimens No: NTP0070, No: NTP0024B and No: NTP0130 respectively (Fig. 10).

Syringic acid, which has been reported from various Iris species, exhibits antibacterial activity against several gram-positive bacteria [40,41]. Liquiritigenin has only been reported from Glycyrrhiza glabra and is described here for the first time in I. pseudacaros [42]. Liquiritigenin has been reported to exhibited significant anti-MRSA activity, which correlates with our activity results [43]. Luteolin 7-O-β-D-glucoside is known for its antimicrobial and antioxidant activity [44,45]. These findings are consistent with previous studies that reveal the bioactivity of compounds in different parts of *I. pseudacorus* [37]. The isolated compounds, as well the mixture of the active compounds was evaluated for their antimicrobial activity against S. aureus ATCC 29213 using the microdilution method. Interestingly, the pure compounds exhibited better antimicrobial activity compared to the 100 % methanolic extracts. The best results were observed with a mixture of the three compounds, that achieved a MIC of 32 µg/mL, clearly revealing a synergistic effect [46,47]. Among the individual compounds, syringic acid showed the least activity with an MIC of 256 $\mu g/mL$ while both luteolin-7-O- β -glucoside and liquiritigenin had a MIC of 128 μ g/mL. Plant extracts are complex mixtures of compounds, and the observed antimicrobial activity of the full extracts may be attributed to antagonistic interactions between different constituents, which could explain why the individual compounds luteolin 7-O-β-D-glucoside and liquiritigenin showed higher activity [48]. Given this complexity, we investigated whether the addition of the three identified compounds would influence the antimicrobial activity of other Iris pseudacorus extracts that initially showed no antimicrobial activity against the tested bacteria.

In a new experiment, we added the individual active compounds, and the mixture of all three to two randomly selected *Iris pseudacorus* samples (voucher specimens No: NTP0022 and NTP0018). The addition of liquiritigenin, luteolin 7-O- β -D-glucoside, and syringic acid did increase the antimicrobial activity of the tested extracts but to a much lower degree than expected. Both voucher specimens No: NTP0022 and NTP0018 exhibited antimicrobial activity upon the addition of the individual compounds and the mixture, but with a MIC of only 512 μ g/mL against both gram positive strains. This raises the question of whether an antagonistic effect is present, given that the extracts alone showed no activity, yet the combination with the extracts resulted in lower activity compared to that of the individual compounds and the mixture.

3.3. Anti-inflammatory and cytotoxicity of active samples and isolated compounds

3.3.1. Effect of Iris extracts and standard compounds on THP-1 cells viability

Building on previous investigations that demonstrated the anti-inflammatory properties of flavonoids in *Iris kashmiriana* [49], the same samples and isolated active compounds were tested for anti-inflammatory effects. Additionally, sample voucher specimens No: NTP0131 was specifically chosen for its interesting chemical profile, as revealed by HPTLC and LC-MS analyses. Following 24 h incubation, none of the four *Iris* extracts showed a significant reduction in THP-1 cell viability at concentrations of 10 and 50 μg /mL. Incubating cells with 100 μg /mL voucher specimens No: NTP0024B *Iris* extract for 24 h

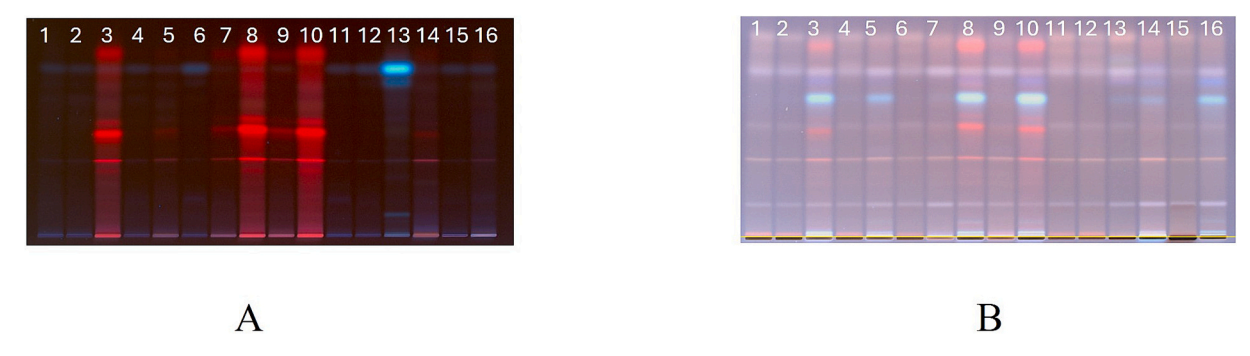


Fig. 8. HPTLC chromatogram of all 16 *Iris* methanol extracts: Mobile phase Toluene: Acetone (1:1), (A) under 366 nm, (B) after derivatization with anisaldehyde sulfuric reagent under UV 366 nm. Lane 1 corresponds to *Iris* extract voucher specimens No: NTP0018, lane 2 NTP0021, lane 3 NTP0022A, lane 4 NTP0022B, lane 5 NTP0022C, lane 6 NTP0023A, lane 7 NTP0023B, lane 8 NTP0023C, lane 9 NTP0024A, lane 10 NTP0024B, lane 11 NTP0024C, lane12 NTP0025, lane 13 NTP 0070, lane 14 NTP0129, lane 15 NTP0130 and lane 16 NTP0131, respectively.

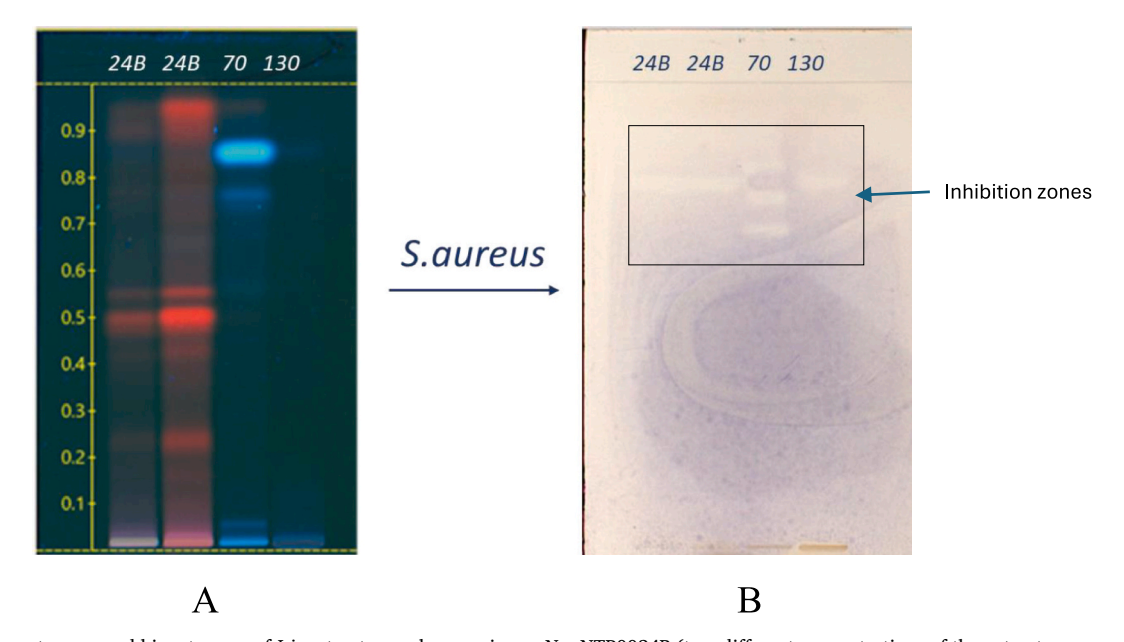


Fig. 9. TLC chromatogram and bioautogram of *Iris* extracts voucher specimens No: NTP0024B (two different concentrations of the extract were applied), NTP0070 and NTP0130. Mobile phase: Toluene: Acetone (1:1). (A) TLC plate after derivatization with anisaldehyde sulfuric reagent under UV 366 nm. (B) TLC-bioautography assay tested against *S. aureus*. The appearance of white areas against a purple-red background on the chromatograms indicates inhibition of bacterial growth. Actively growing microorganisms can reduce INT to a purple-red colour [57]. (For interpretation of the references to colour in this figure legend, the reader is referred to the web version of this article.)

Fig. 10. Identified active compounds by bioautography: (A) syringic acid for voucher specimens No: NTP0024B, (B) liquiritigenin for voucher specimens No: NTP0070 and (C) luteolin 7-O-β-D-glucoside for NTP0130.

resulted in a significant reduction in THP-1 cells viability when compared with control and cells treated with LPS alone (Fig. 11A and B). Likewise, none of the tested standard compounds had a significant

impact on cell viability implying that the cytotoxic effect of voucher specimens No: NTP0024B extract is very likely not attributable to any of these compounds. Given the complex nature of plant extracts the

Cytotoxicity test

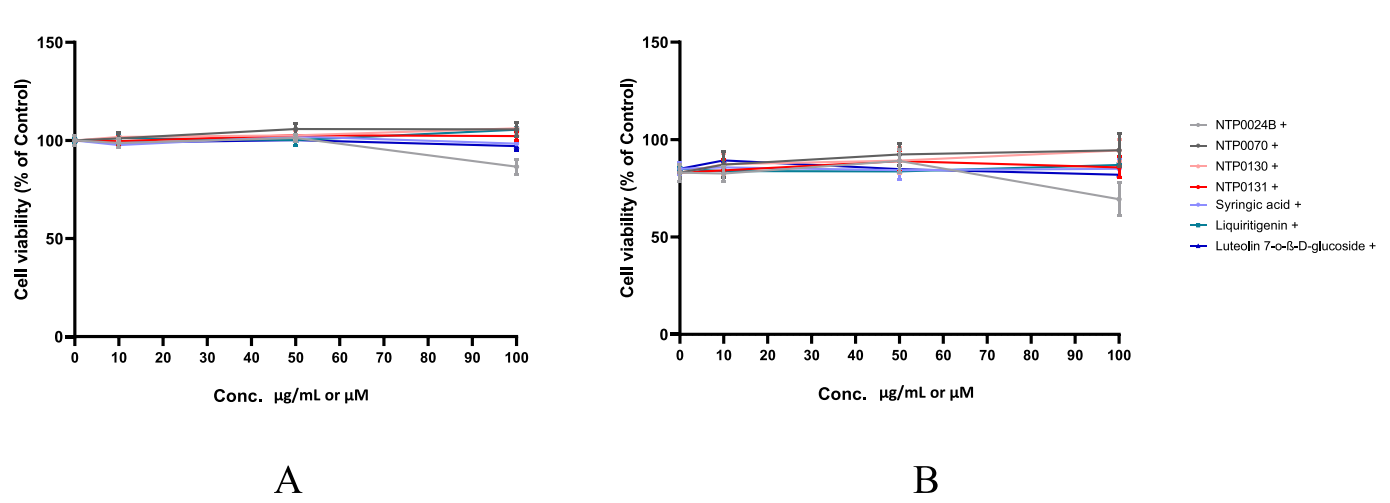


Fig. 11. Effect of *Iris* extracts and standards compounds on THP-1 cells' viability. Treating THP-1 cells to various concentration of *Iris* extracts and standards compounds for 24 h in the absence (A) or presence of LPS (B) resulted in no significant change in cells' viability apart from significant reduction in viability caused by 24 h incubation with 100 μ g /ml of voucher specimens No: NTP0024B *Iris* extract in comparison with control cells. Data represent means \pm SD from three independent experiments, *P < 0.05, **P < 0.01 compared to controls or LPS alone.

cytotoxic activity observed with voucher specimens No: NTP0024B extract could be due to the presence of other cytotoxic compounds and/or a synergistic effect between components. In line with this it has been suggested that tannin constituents of *Iris pseudacorus* rhizome extract are responsible for its cytotoxic activity towards MCF-7 cell [10,50].

3.3.2. The anti-inflammatory profile of Iris extracts and standard compounds

In addition, to the previously described activities the potential capacity of the extracts and standard compounds to suppress an inflammatory response induced by LPS was investigated.

The innate immune system provides a prompt immunosurveillance against pathogens and coordinate with adaptive immune system to initiate an antigen-specific response. However, any abnormal activation

of the innate immune system causes detrimental inflammatory responses [51]. LPS, a major component of bacterial cell membrane, is a well-characterised inducer of the inflammatory response via activation of toll-like receptor 4 (TLR4) [51]. Thus, it was used in this study to initiate an inflammatory response and to activate THP-1 cells to secrete proinflammatory cytokines (i.e., TNF- α , IL-6, IL-1 β and Rantes).

The potential anti-inflammatory effect of *Iris* extracts and standard compounds was examined by testing the level of IL-6, TNF- α , IL-1 β and Rantes in cell culture media supernatants collected from THP-1 cells treated with 100 μ g/mL of voucher specimens No: NTP0070, NTP0130 and NTP0131 as well as 100 μ M of the three standard compounds in the presence or absence of LPS. Due to a significant reduction in cell viability induced by 24 h incubation with 100 μ g/mL of voucher specimens No: NTP0024B extract, the levels of four cytokines in

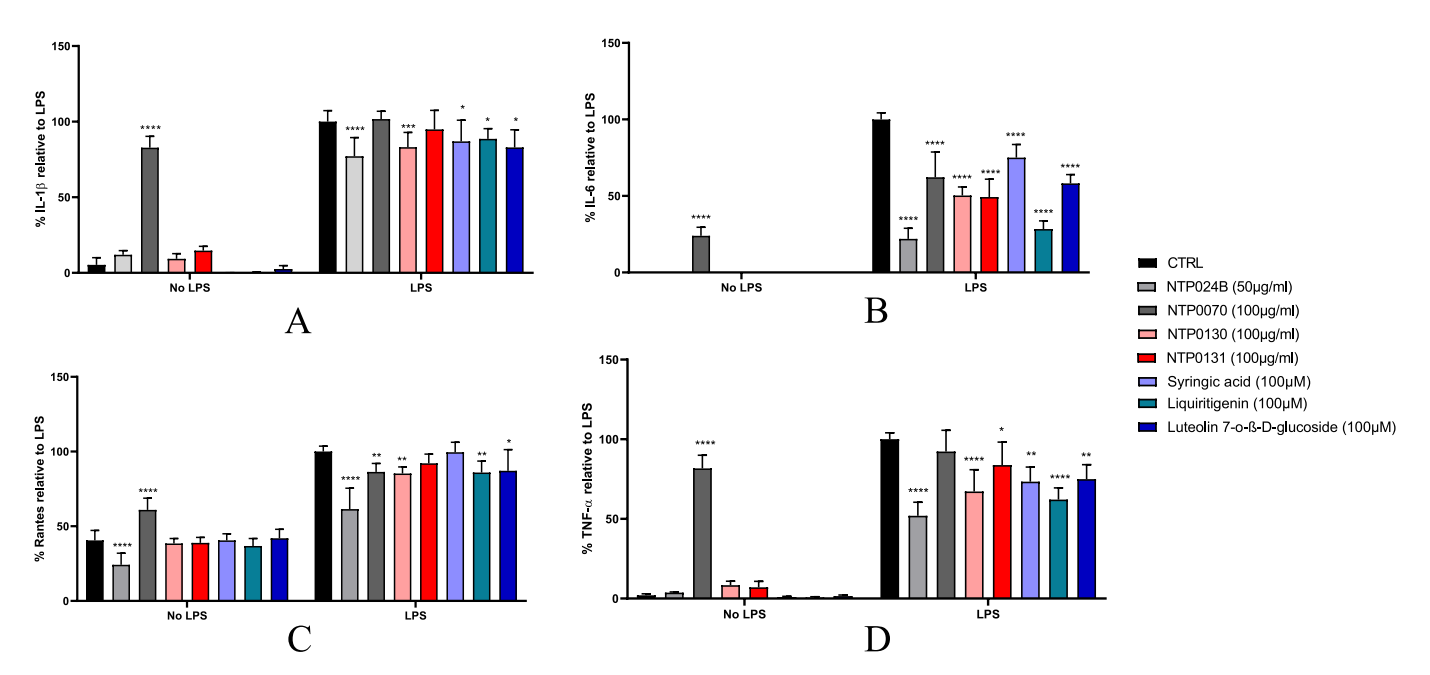


Fig. 12. The anti-inflammatory profile of *Iris* extracts and standard compounds. The level of four cytokines in supernatants collected from THP-1 cells treated with various *Iris* extract and standard compounds for 24 h in the presence or absence LPS. Data represent means \pm SD from three independent experiments, *P < 0.05, **P < 0.01, *** P < 0.001 compared to control (with or without LPS).

supernatants collected from cells treated with 50 $\mu g/mL$ of the latter extract were tested.

Treating cells with all the four *Iris* extracts and the three standard compounds significantly (p < 0.001) attenuated the LPS induced rise in IL-6 level. Voucher specimens No: NTP0024B extract and liquiritigenin standard compound had the most pronounced inhibitory effect (Fig. 12A).

Treatment with voucher specimens No: NTP0024B and NTP0130 extracts as well as the three standard compounds, caused significant inhibition in the LPS-induced increase in TNF- α and IL-1 β levels. However, voucher specimens No: NTP0070 and NTP0131 extracts had no significant suppressor effect (Fig. 12B and C). The trend was, to some extent, different with Rantes level. Three extracts (i.e., voucher specimens No: NTP0024B, NTP0070 and NTP0130) and two standards (i.e., liquiritigenin and luteolin 7-O- β -D-glucoside) caused significant suppression in LPS-induced increase in Rantes level, whereas voucher specimens No: NTP0131 extract and syringic acid had no inhibitory effect (Fig. 12D).

Treatment with voucher specimens No: NTP0070 extract without LPS resulted in a significant increase (p < 0.001) in all tested cytokines (Fig. 11A-D). NTP0024B extract, on the other hand, caused a significant reduction in Rantes level when compared with the control (Fig. 12D).

The main target of all extracts was LPS-induced IL-6 secretion, and its levels was reduced significantly by the treatment with all *Iris* extracts as compared with LPS alone (Fig. 12A). As mentioned before, the other cytokines were also suppressed by *Iris* extracts but to a lesser extent than IL-6 (Fig. 12B-D). It is important to note that the, extract of Iris leaves (i. e., voucher specimens No: NTP0024B) had the most powerful inhibitory effect on all cytokines. The analysis of LC-MS data (Supplementary Table 2) revealed that all the *Iris* extracts tested contain numerous flavonoids including syringic acid, liquiritigenin and luteolin 7-O- β -D-glucoside. Flavonoids possess numerous pharmacological activities including anti-microbial and anti-inflammatory effects [25,52,53]. Thus, it is conceivable that the anti-inflammatory effect of *Iris* extracts observed in this study can be attributed to these flavonoid components t and to a potentially a synergistic effect between these bioactive compounds.

Our data revealed that the three standards of the flavonoids investigated (i.e., syringic acid, liquiritigenin and luteolin 7-O-β-D-glucoside) possess anti-inflammatory effects as they all suppressed LPS-induced IL-6 secretion and, to a lesser extent, the other three cytokines with liguiritigenin having the most powerful effect (Fig. 12). These findings are in agreement with previous studies that have demonstrated that these compounds possess anti-inflammatory effects. For instance, liquiritigenin, which is a dihydroxyflavanone compound, has been shown to suppress high glucose [54] and high fructose-induced [55] inflammatory cytokine release by targeting the nuclear factor-kappa B (NF-κB) signalling pathway in vitro and in vivo [56]. Syringic acid has also been shown to exert anti-inflammatory effect through down-regulation of a number of genes involved in inflammation including NF-κB [41,57,58]. Moreover, in vitro and in silico studies have revealed that syringic acid can inhibit the activity of phospholipase A2 enzyme which plays an important role in the inflammatory pathways [59]. Likewise, luteolin 7-O-β-D-glucoside, which is a glycosyloxyflavone with antioxidant and anti-inflammatory activities [52,60], has been demonstrated to inhibit proinflammatory genes' transcription by supressing the translocation of phosphorylated signal transducer and activator of transcription 3 (STAT3) from cytoplasm to the nucleus [61,62]. Moreover, it increases the production of cortisol which also contributes to its antiinflammatory activity [61,62].

4. Conclusion

This study achieved its primary objective of untargeted chemical profiling and biological activity testing of extracts of various parts of *Iris pseudacorus* and locations in Ireland. Comprehensive profiling using ¹H

NMR, HPTLC, and LC-MS allowed the identification of numerous compounds, particularly flavonoids, that varied significantly between the parts of the plant and collection sites.

 1 H NMR analysis revealed characteristic signals for phenolic compounds, flavonoid glycosides, isoflavonoids, and primary metabolites in all *Iris* samples. OPLS modelling confirmed that these metabolites were significantly influenced by the plant part and region of collection, with validated statistical robustness ($Q^{2} = 0.933$, *p*-value <0.05).

GC–MS analysis identified 108 metabolites, with distinct marker compounds associated with different plant organs and, to a lesser extent, collection locations. Key distinctive metabolites between leaves and stems and rhizomes included tagatose, glucaric acid, and fructose, among others. In contrast, rhizomes were characterised by markers such as glucosamine and loganin. The effect of collection location on metabolite variation was minimal.

UHPLC-MS analysis, combined with feature based molecular networking via GNPS, allowed the identification of 73 metabolites in *Iris* samples, including specialised metabolites such as flavonoids, isoflavonoids, and alkaloids. Similarly to the GC–MS and ¹H NMR analyses, metabolic variation was more pronounced between plant organs than between collection locations. Marker compounds for leaves, stems, and rhizomes were identified, with distinct metabolites such as isoflavonoids in stems and tannins in rhizomes. Additionally, irisolidone and methyl syringate were identified as markers for Kildare samples, while no distinct metabolites were linked to Donegal samples. The data confirmed significant metabolic differences based on both plant organs and collection sites.

The antimicrobial assays showed that certain *Iris pseudacorus* extracts (voucher specimens No: NTP0024B, NTP0070 and NTP0130) exhibited activity against *Staphylococcus aureus* ATCC 29213. Using direct bio-autography and subsequent LC-MS active compounds, such as liquiritigenin, syringic acid, and luteolin 7-O- β -D-glucoside were identified. Notably, these pure compounds displayed better activity compared to the whole methanol extracts, suggesting possible antagonistic interactions within the complex mixtures of the extracts.

All tested extracts and standard compounds demonstrated significant anti-inflammatory effects, particularly in reducing IL-6 levels, with liquiritigenin showing the most potent activity.

These findings underscore the potential of *Iris pseudacorus* as a source of bioactive compounds with antimicrobial and anti-inflammatory properties supporting ethnomedical use. The complex interplay of components within the extracts highlights the importance of considering whole extracts in addition to isolated compounds for potential therapeutic applications.

CRediT authorship contribution statement

Özlem Erol: Writing – review & editing, Writing – original draft, Visualization, Software, Methodology, Data curation, Conceptualization. Shipra Nagar: Writing – review & editing, Writing – original draft, Project administration, Methodology. Mohammed Ali Selo: Writing – review & editing, Writing – original draft, Visualization, Methodology, Data curation. Ismael Obaidi: Writing – review & editing, Writing – original draft, Methodology, Data curation. John J. Walsh: Project administration, Supervision. Helen Sheridan: Writing – review & editing, Funding acquisition. Young Hae Choi: Writing – review & editing, Visualization, Software, Data curation, Conceptualization.

Funding

This research was funded by the Unlocking Nature's Pharmacy from Bogland Species (UNPBS) Project under grant number DOJProject209825, funded by the Department of Justice, Ireland.

Declaration of competing interest

The authors declare no conflict of interest. The funders had no role in the design of the study, in the collection, analyses, or interpretation of data; in the writing of the manuscript; or in the decision to publish the results.

Acknowledgements

We would like to acknowledge John J. Cannon from Teagasc, the Agriculture and Food Development Authority of Ireland for providing the twelve out of sixteen *Iris pseudacorus* plant samples for this research. We would further like to thank Shilong Chen, NatPro Centre, School of Pharmacy and Pharmaceutical Sciences, Trinity College Dublin, for performing extractions and sample preparation for cell viability and anti-inflammatory study.

Appendix A. Supplementary data

Supplementary data to this article can be found online at https://doi.org/10.1016/j.fitote.2025.106671.

Data availability

LCMS raw data is available in the MAssIVE respository and the link to the GNPS2 molecular network is also now available in the revised version

References

- [1] J. Feehan, G. O'Donovan, F. Renou-Wilson, D. Wilson, The Bogs of Ireland: An Introduction to the Natural, Cultural and Industrial Heritage of Irish Peatlands, University College Dublin. Environmental Institute, 2008. http://hdl.handle. net/10197/12228.
- [2] W. Ediviani, C.R. Priadi, S.S. Moersidik, Nutrient uptake from liquid digestate using ornamental aquatic macrophytes (*Canna indica, Iris pseudacorus, Typha latifolia*) in a constructed wetland system, in: Journal of Physics: Conference Series vol. 1022, No. 1, IOP Publishing, 2018, p. 012052.
- [3] D.E. Allen, G. Hatfield. Medicinal Plants in Folk Tradition: An Ethnobotany of Britain & Ireland, Timber Press, Cambridge, 2004.
- [4] Dúchas.ie, Text search [online] Available at: https://www.duchas.ie/en/src? q=yellow+iris [Accessed 24 Nov. 2021].
- [5] A.Ž. Kostić, U.M. Gašić, M.B. Pešić, S.P. Stanojević, M.B. Barać, M.P. Mačukanović-Jocić, S.N. Avramov, Ž.L. Tešić, Phytochemical analysis and Total antioxidant capacity of rhizome, above-ground vegetative parts and flower of three Iris species, Chem. Biodivers. 16 (3) (2019) e1800565, https://doi.org/10.1002/ chdy.201800565
- [6] W. Kukula-Koch, E. Sieniawska, J. Widelski, et al., Major secondary metabolites of Iris spp, Phytochem. Rev. 14 (2015) 51–80, https://doi.org/10.1007/s11101-013-9333-1
- [7] M.M. Okba, P.M.A. Baki, M. Abu-Elghait, A.M. Shehabeldine, M.M. El-Sherei, A. E. Khaleel, M.A. Salem, UPLC-ESI-MS/MS profiling of the underground parts of common *Iris* species in relation to their anti-virulence activities against Staphylococcus aureus, J. Ethnopharmacol. 282 (2022) 114658.
- [8] H.G. Sary, N.A. Ayoub, A.B. Singab, A.H. Ahmed, M.M. Al-Azizi, Chemical constituents and molluscicidal activity of *Iris pseudacorus L.* cultivated in Egypt, Bull. Pharm. Sci. Assiut 27 (1) (2004) 161–169.
- [9] M. Ramtin, A. Massiha, K.P.M.R. Majid, K. Issazadeh, M. Assmar, S. Zarrabi, In vitro antimicrobial activity of *Iris pseudacorus* and *Urtica dioica*, Zahed. J. Res. Med. Sci. 16 (3) (2014) 35–39.
- [10] A. Michalak, M. Krauze-Baranowska, P. Migas, A. Kawiak, A. Kokotkiewicz, A. Królicka, *Iris pseudacorus* as an easily accessible source of antibacterial and cytotoxic compounds, J. Pharm. Biomed. Anal. 195 (2021) 113863.
- [11] B. Sener, D. Sevim, Discovery of bioactive drug candidates from some Turkish medicinal plants-neuroprotective potential of *Iris pseudacorus L*, Pure Appl. Chem. 92 (7) (2020) 1175–1179.
- [12] D.V. Tarbeeva, S.A. Fedoreev, M.V. Veselova, A.I. Kalinovskii, P.G. Gorovoi, Polyphenolic metabolites from *Iris pseudacorus*, Chem. Nat. Compd. 50 (2) (2014) 363–365.
- [13] D.V. Tarbeeva, S.A. Fedoreev, M.V. Veselova, A.I. Kalinovskii, P.G. Gorovoi, O. S. Vishchuk, S.P. Ermakova, P.A. Zadorozhnyi, Polyphenolic metabolites from *Iris pseudacorus* roots, Chem. Nat. Compd. 51 (3) (2015) 451–455.
- [14] J.L. Kim, H.M. Li, Y.H. Kim, Y.J. Lee, J.H. Shim, S.S. Lim, Y.H. Kang, Osteogenic activity of yellow flag iris (*Iris pseudacorus*) extract modulating differentiation of osteoblasts and osteoclasts, Am. J. Chin. Med. 40 (06) (2012) 1289–1305.

- [15] S. Huwaitat, E. Al-Khateeb, S. Finjan, Isolation and identification of some phytochemical compounds from different parts of *Iris nigricans*, Eur. Sci. J. 9 (2013) 213–218.
- [16] A. Alam, V. Jaiswal, S. Akhtar, B.S. Jayashree, K.L. Dhar, Isolation of isoflavones from *Iris kashmiriana* baker as potential anti proliferative agents targeting NFkappaB, Phytochemistry 136 (2017) 70–80, https://doi.org/10.1016/j. phytochem.2017.01.002.
- [17] T. Mackul'ak, M. Mosný, J. Škubák, R. Grabic, L. Birošová, Fate of psychoactive compounds in wastewater treatment plant and the possibility of their degradation using aquatic plants, Environ. Toxicol. Pharmacol. 39 (2) (2015) 969–973.
- [18] Y. Zhang, T. Lv, P.N. Carvalho, C.A. Arias, Z. Chen, H. Brix, Removal of the pharmaceutical's ibuprofen and iohexol by four wetland plant species in hydroponic culture: plant uptake and microbial degradation, Environ. Sci. Pollut. Res. 23 (3) (2016) 2890–2898.
- [19] A.I. Machado, R. Fragoso, A.V. Dordio, E. Duarte, Performance of *Iris pseudacorus* and *Typha domingensis* for furosemide removal in a hydroponic system, Int. J. Phytoremed. 22 (8) (2020) 863–871.
- [20] T. Lv, Y. Zhang, M.E. Casas, P.N. Carvalho, C.A. Arias, K. Bester, H. Brix, Phytoremediation of imazalil and tebuconazole by four emergent wetland plant species in hydroponic medium, Chemosphere 148 (2016) 459–466.
- [21] X.Y. Tang, Y. Yang, M.B. McBride, R. Tao, Y.N. Dai, X.M. Zhang, Removal of chlorpyrifos in recirculating vertical flow constructed wetlands with five wetland plant species, Chemosphere 216 (2019) 195–202.
- [22] Q. Wang, W. Zhang, C. Li, B. Xiao, Phytoremediation of atrazine by three emergent hydrophytes in a hydroponic system, Water Sci. Technol. 66 (6) (2012) 1282–1288
- [23] A. Parzych, M. Cymer, K. Macheta, Leaves and roots of *Typha latifolia L*. and *Iris pseudacorus L*. as bioindicators of contamination of bottom sediments by heavy metals, Limnol. Rev. 16 (2) (2016) 77.
- [24] C. Pérez-Sirvent, C. Hernández-Pérez, M.J. Martínez-Sánchez, M.L. García-Lorenzo, J. Bech, Metal uptake by wetland plants: implications for phytoremediation and restoration, J. Soils Sediments 17 (5) (2017) 1384–1393.
- [25] S.J. Maleki, J.F. Crespo, B. Cabanillas, Anti-inflammatory effects of flavonoids, Food Chem. 299 (2019) 125124. PMID: 31288163, https://doi.org/10.1016/j. foodchem.2019.125124.
- [26] Jackson Peter Wyse, Missouri Botanical Garden and National Botanic Gardens (Ireland) (2014). Ireland's Generous Nature: The Past and Present Uses of Wild Plants in Ireland. St. Louis, Missouri: Missouri Botanical Garden Press; Glasnevin, Dublin. Ireland.
- [27] CLSI, Performance Standards for Antimicrobial Susceptibility Testing. CLSI Supplement M100, 32nd ed, Clinical and Laboratory Standards Institute, Wayne, PA, 2022.
- [28] M. Ghasemi, T. Turnbull, S. Sebastian, I. Kempson, The MTT assay: utility, limitations, pitfalls, and interpretation in bulk and single-cell analysis, Int. J. Mol. Sci. 22 (23) (2021) 12827, https://doi.org/10.3390/ijms222312827.
- [29] M. Chambers, B. Maclean, R. Burke, et al., A cross-platform toolkit for mass spectrometry and proteomics, Nat. Biotechnol. 30 (2012) 918–920, https://doi. org/10.1038/nbt.2377.
- [30] R. Schmid, S. Heuckeroth, A. Korf, et al., Integrative analysis of multimodal mass spectrometry data in MZmine 3, Nat. Biotechnol. 41 (2023) 447–449, https://doi. org/10.1038/s41587-023-01690-2.
- [31] MetaboScape 4.0 Untargeted Metabolomics solution. Bruker.com. Available at: https://www.bruker.com/products/mass-spectrometry-and-separations/ms-s oftware/metaboscape.
- [32] M. Wang, et al., Sharing and community curation of mass spectrometry data with global natural products social molecular networking, Nat. Biotechnol. 34 (2016) 828–837, https://doi.org/10.1038/nbt.3597.
- [33] A.A. Aksenov, et al., Algorithmic learning for auto-deconvolution of GC-MS data to enable molecular networking within GNPS, bioRxiv (2020), https://doi.org/ 10.1101/2020.01.13.905091, 2020.01.13.905091.
- [34] O. Mykhailenko, Z. Gudžinskas, V. Kovalyov, V. Desenko, L. Ivanauskas, I. Bezruk, V. Georgiyants, Effect of ecological factors on the accumulation of phenolic compounds in *Iris* species from Latvia, Lithuania and Ukraine, Phytochem. Anal. 31 (5) (2020) 545–563.
- [35] B.D. Moore, E. Isidoro, J.R. Seemann, Distribution of 2-carboxyarabinitol among plants, Phytochemistry 34 (3) (1993) 703–707. ISSN 0031–9422, https://doi. org/10.1016/0031-9422(93)85343-P.
- [36] F. Hanawa, S. Tahara, J. Mizutani, Isoflavonoids produced by Iris pseudacorus leaves treated with cupric chloride, Phytochemistry 30 (1) (1991) 157–163, https://doi.org/10.1016/0031-9422(91)84117-.
- [37] A.N.B. Singab, I.M. Ayoub, M. El-Shazly, M. Korinek, T.Y. Wu, Y.B. Cheng, F.-R. Chang, Y.C. Wu, Shedding the light on Iridaceae: ethnobotany, phytochemistry and biological activity, Ind. Crop. Prod. 292 (2016) 308–335, https://doi.org/10.1016/j.indcrop.2016.07.040.
- [38] L.F. Salomé-Abarca, C.A.M.J.J. van den Hondel, Ö. Erol, P.G.L. Klinkhamer, H. K. Kim, Y.H. Choi, HPTLC-based chemical profiling: an approach to monitor plant metabolic expansion caused by fungal endophytes, Metabolites 11 (3) (2021) 174, https://doi.org/10.3390/metabo11030174 (PMID: 33802951; PMCID: PMC8002819).
- [39] B.L.T. Nguyen, C. Palmieri, K.T.T. Nguyen, D. Le, T.T. Ngo, C.K. Tran, H. Q. Nguyen, H.T. Pham, M. Muller, P. Duez, A. Nachtergael, HPTLC fingerprinting and cytotoxicity of secondary metabolites of *Equisetum Diffusum D*. Don extracts, Intern. J. Plant, Animal Environ. Sci. 11 (2021) 596–613.
- [40] C. Srinivasulu, M. Ramgopal, G. Ramanjaneyulu, C.M. Anuradha, Kumar C. Suresh, Syringic acid (SA) – a review of its occurrence, biosynthesis, pharmacological and

- industrial importance, Biomed. Pharmacother. 2108 (2018) 547–557, https://doi.org/10.1016/j.biopha.2018.09.069.
- [41] S. Khatib, C. Faraloni, L. Bouissane, Exploring the use of *Iris* species: antioxidant properties, phytochemistry, medicinal and industrial applications, Antioxidants 11 (2022) 526, https://doi.org/10.3390/antiox11030526.
- [42] Y.W. Chin, H.A. Jung, Y. Liu, B.N. Su, J.A. Castoro, W.J. Keller, M.A. Pereira, Antioxidant constituents of the roots and stolons of licorice (*Glycyrrhiza glabra*), J. Agric. Food Chem. 55 (12) (2007) 4691–4697.
- [43] R. Gaur, V.K. Gupta, P. Singh, A. Pal, M.P. Darokar, R.S. Bhakuni, Drug resistance reversal potential of Isoliquiritigenin and Liquiritigenin isolated from Glycyrrhiza glabra against methicillin-resistant Staphylococcus aureus (MRSA), Phytother. Res. 30 (2016) 1708–1715, https://doi.org/10.1002/ptr.5677. 13;55(12):4691-7. 10.1021/jf0703553.
- [44] I. Górniak, R. Bartoszewski, J. Króliczewski, Comprehensive review of antimicrobial activities of plant flavonoids, Phytochem. Rev. 18 (2019) 241–272, https://doi.org/10.1007/s11101-018-9591-z.
- [45] L.T.T. Nguyen, T.T. Nguyen, H.N. Nguyen, Q.T.P. Bui, Analysis of active compounds and bioactivity of leaves extracts of *Sonneratia* species, Eng. Rep. (2024) e12870, https://doi.org/10.1002/eng2.12870.
- [46] S. Van Vuuren, A. Viljoen, Plant-based antimicrobial studies _ methods and approaches to study the interaction between natural products, Planta Med. 77 (11) (2011) 1168–1182, https://doi.org/10.1055/s-0030-1250736.
- [47] N. Vaou, E. Stavropoulou, C.C. Voidarou, Z. Tsakris, G. Rozos, C. Tsigalou, E. Bezirtzoglou, Interactions between medical plant-derived bioactive compounds: focus on antimicrobial combination effects, Antibiotics 11 (8) (2022) 1014, https://doi.org/10.3390/antibiotics11081014.
- [48] L.K. Caesar, N.B. Cech, Synergy and antagonism in natural product extracts: when 1 + 1 does not equal 2, Nat. Prod. Rep. 36 (6) (2019) 869–888, https://doi.org/ 10.1039/c9np00011a (PMID: 31187844; PMCID: PMC6820002).
- [49] N. Nighat, Immunomodulatory activity of isoflavones isolated from *Iris kashmiriana*: effect on T-lymphocyte proliferation and cytokine production in Balb/c mice, Biomed. Prev. Nutr. 3 (2) (2013) 151–157. ISSN 2210-5239, https://doi.org/10.1016/j.bionut.2012.12.006.
- [50] X. Chen, X. Zhang, C. Geng, T. Li, J. Chen, New C16-noriridals and formyl-monocycloiridals from the rhizomes of *Iris pseudoacorus*, Fitoterapia 124 (2018) 160–166.
- [51] X. Zhang, G. Wang, E.C. Gurley, H. Zhou, Flavonoid apigenin inhibits lipopolysaccharide-induced inflammatory response through multiple mechanisms in macrophages, PLoS One 9 (9) (2014) e107072.

- [52] C. Zaragozá, L. Villaescusa, J. Monserrat, F. Zaragozá, M. Álvarez-Mon, Potential therapeutic anti-inflammatory and immunomodulatory effects of Dihydroflavones, flavones, and Flavonols, Molecules 25 (4) (2020).
- [53] J.M. Al-Khayri, G.R. Sahana, P. Nagella, B.V. Joseph, F.M. Alessa, M.Q. Al-Mssallem, Flavonoids as potential anti-inflammatory molecules: a review, Molecules 27 (9) (2022).
- [54] X. Zhu, J. Shi, H. Li, Liquiritigenin attenuates high glucose-induced mesangial matrix accumulation, oxidative stress, and inflammation by suppression of the NFκB and NLRP3 inflammasome pathways, Biomed. Pharmacother. 106 (2018) 976–982.
- [55] X.W. Xie, Liquiritigenin attenuates cardiac injury induced by high fructose-feeding through fibrosis and inflammation suppression, Biomed. Pharmacother. 86 (2017) 694-704
- [56] A. Keranmu, L.B. Pan, J. Fu, P. Han, H. Yu, Z.W. Zhang, H. Xu, X.Y. Yang, J.C. Hu, H.J. Zhang, M.M. Bu, J.D. Jiang, N.Z. Xing, Y. Wang, Biotransformation of Liquiritigenin into characteristic metabolites by the gut microbiota, Molecules 27 (10) (2022).
- [57] P. Dey, S. Roy Chowdhuri, M.P. Sarkar, T.K. Chaudhuri, Evaluation of antiinflammatory activity and standardisation of hydro-methanol extract of underground tuber of *Dioscorea alata*, Pharm. Biol. 54 (8) (2016) 1474–1482.
- [58] J.R. Ham, H.-I. Lee, R.-Y. Choi, M.-O. Sim, K.-I. Seo, M.-K. Lee, Anti-steatotic and anti-inflammatory roles of syringic acid in high-fat diet-induced obese mice, Food Funct. 7 (2) (2016) 689–697.
- [59] K.V. Dileep, C. Remya, J. Cerezo, A. Fassihi, H. Pérez-Sánchez, C. Sadasivan, Comparative studies on the inhibitory activities of selected benzoic acid derivatives against secretory phospholipase A2, a key enzyme involved in the inflammatory pathway, Mol. BioSyst. 11 (7) (2015) 1973–1979.
- [60] A. De Stefano, S. Caporali, N. Di Daniele, V. Rovella, C. Cardillo, F. Schinzari, M. Minieri, M. Pieri, E. Candi, S. Bernardini, M. Tesauro, A. Terrinoni, Antiinflammatory and proliferative properties of Luteolin-7-O-glucoside, Int. J. Mol. Sci. 22 (3) (2021).
- [61] R. Palombo, I. Savini, L. Avigliano, S. Madonna, A. Cavani, C. Albanesi, A. Mauriello, G. Melino, A. Terrinoni, Luteolin-7-glucoside inhibits IL-22/STAT3 pathway, reducing proliferation, acanthosis, and inflammation in keratinocytes and in mouse psoriatic model, Cell Death Dis. 7 (8) (2016) e2344.
- [62] W.J.M. Begue, R.M. Kline, The use of tetrazolium salts in bioautographic procedures, J. Chromatogr. 64 (1) (1972) 182–184, https://doi.org/10.1016/ s0021-9673(00)92965-0.